Phylogenetic Relationships among Fantail Darters (Percidae: *Etheostoma: Catonotus*): Total Evidence Analysis of Morphological and Molecular Data

JEAN C. PORTERFIELD, LAWRENCE M. PAGE, AND THOMAS J. NEAR

Results of a phylogenetic analysis of the complete mitochondrial cytochrome *b* gene (1140 base pairs) for all species of *Catonotus* are presented along with a synthesis and phylogenetic analysis of published morphological data. The two datasets are combined in a total evidence analysis, and results from the molecular, morphological, and total evidence datasets are compared with each other and with previously published hypotheses. Phylogenetic relationships suggested by morphological data are similar to those from previous studies. The cytochrome *b* and total evidence analyses also produced trees that are generally congruent with previous hypotheses. The monophyly of the *Etheostoma squamiceps* group and the monophyly of a clade including members of the *E. virgatum* and *E. flabellare* groups are well supported. However, in contrast to traditional classification, *E. barbouri* usually clustered with the *E. flabellare* group, and *E. percnurum* usually clustered with the *E. virgatum* group. *Etheostoma percnurum* and *E. barbouri* possess many autapomorphies, and it is possible that they share fewer cytochrome *b* characters with close relatives than they share with other species due to homoplasy resulting from accelerated rates of evolution. Also, in contrast to earlier hypotheses, the molecular and total evidence analyses suggested that *E. squamiceps, E. crossopterum,* and *E. olivaceum* are closely related. An earlier hypothesis based on morphology suggested that *E. olivaceum* was basal to other members of the *E. squamiceps* group and that *E. squamiceps* was related to *E. chienense, E. pseudovulatum, E. oophylax,* and *E. neopterum. Etheostoma olivaceum* has been considered basal because it lacks putative synapomorphies of all other members of the *E. squamiceps* group. Although reversals (in *E. olivaceum*) and convergence (in *E. squamiceps*) in character states are possible, a test of the two hypotheses of relationship requires additional data.

FANTAIL darters have been the subject of several systematic studies since Bailey and Gosline (1955) hypothesized their monophyly and placed them in the subgenus *Catonotus* of *Etheostoma.* Kuehne and Small (1971) diagnosed the subgenus, which subsequently was modified by Braasch and Page (1979) and Page (1981). Phylogenetic relationships have been hypothesized using external morphological characters by Braasch and Mayden (1985), Page (1985), and Page et al. (1992). Page (1985) analyzed behavioral and morphological data on the 10 described species. Braasch and Mayden (1985) analyzed a dataset consisting of 44 external morphological and behavioral characters and described two additional species. Page et al. (1992) used nine external morphological characters to investigate relationships among the *E.*

squamiceps species group, and described five species. Jenkins (Jenkins and Burkhead, 1994) described *Etheostoma percnurum,* the 18th species to be recognized in the subgenus.

Egg-clustering breeding behavior (Page 1985) and several forms of egg mimics (Page and Swofford, 1984; Knapp and Sargent, 1989; Page and Bart, 1989) make species of *Catonotus* one of the most morphologically and behaviorally interesting assemblages of North American fishes and a prime target for studying character evolution. Most species of *Catonotus* have small ranges in the Eastern Highlands of the southeastern United States; only *E. flabellare* is widely distributed in eastern North America (Braasch and Mayden, 1985; Page et al., 1992; Jenkins and Burkhead, 1994).

Although morphological features of *Catonotus*

species have been well studied, they may not contain enough phylogenetic information to assess relationships. Problems include too few characters, homoplasy (especially in meristic characters), and lack of character independence. When confronted with similar problems in other taxa, researchers have turned to molecular data for augmentation of morphological datasets (e.g., Alves-Gomes et al., 1995; Miyamoto, 1996). In general, the analysis of DNA sequence data has proven to be an effective tool for resolving species-level phylogenies (Hillis et al., 1996).

Combining datasets to estimate phylogenetic relationships, that is, using the total evidence approach (Kluge, 1989), assumes that the analysis of all available data provides the best estimate of phylogenetic history. One potential benefit of this approach is the positive interaction of datasets that are informative at different phylogenetic levels (Hillis, 1987). The combined analysis of molecular and morphological data has been extensively examined, both in review papers (e.g., Swofford, 1991; Larson, 1994; Huelsenbeck et al., 1996) and in empirical studies (e.g., Dimmick and Larson, 1996; Poe, 1996; Messenger and McGuire, 1998). One popular conclusion is that it is advisable to assess the congruence of datasets before combining them (e.g., Bull et al., 1993). Methods for evaluating dataset congruence include calculating incongruence indices (Mickevich and Farris, 1981; Miyamoto in Kluge, 1989), testing for statistically significant differences between tree lengths (e.g., Templeton, 1983), and performing partition-homogeneity tests (Farris et al., 1995).

We present the results of a phylogenetic analysis of the complete mitochondrial cytochrome *b* gene for all species of *Catonotus* and a synthesis and phylogenetic analysis of available morphological data. The two datasets are combined in a total evidence analysis, and results from the molecular, morphological, and total evidence datasets are compared with each other and with previously published hypotheses.

MATERIALS AND METHODS

Species examined.—The 18 species of *Catonotus* are placed in three species groups (Page, 1985): the *E. flabellare* group (fantails), the *E. virgatum* group (barcheeks), and the *E. squamiceps* group (spottails). The *E. flabellare* group includes the widespread and variable nominal species, *E. kennicotti*, and *E. percnurum.* The *E. virgatum* group is characterized by a distinct pigment bar on the cheek and contains five species: *E. barbouri, E. obeyense, E. smithi, E. striatulum,* and *E. virgatum.*

TABLE 1.   SEQUENCES FOR PRIMERS USED IN PCR AMPLIFICATION AND SEQUENCING. All primers were designed by the authors.

Primer	Sequence (5' to 3')
GLU	GAC TTG AAG AAC CAC CGT TG
307F	TAY TAY GGM TCY TAY CTY TAY A
658F	TTY CAY CCY TAY TTY TCY TA
401R	CAG GGG AGN ACA TAV CCW AC
683R	TCY TTR TAG GAG AAG TAN GGG TG
768R	ACH ARD GGR TTD GCD GGG GT
THR	TCC GAC ATT CGG TTT ACA AG

The largest species group is the *E. squamiceps* group with 10 species: *E. chienense, E. corona, E. crossopterum, E. forbesi, E. nigripinne, E. neopterum, E. olivaceum, E. oophylax, E. pseudovulatum,* and *E. squamiceps.*

DNA sequences were obtained for the complete mitochondrial cytochrome *b* gene (1140 base pairs) for 16 species of *Catonotus* and one outgroup taxon, *E. parvipinne.* Sequences for two other *Catonotus* species, *E. flabellare* and *E. kennicotti,* and for 18 outgroup taxa were taken from Song et al. (1998).

DNA sequence data.—Total DNA was isolated from frozen or ethanol-preserved muscle tissue using standard proteinase-K digestion and phenol-chloroform extraction methods. Primers GLU and THR were used for double-stranded polymerase chain reaction (PCR) amplification with the following conditions: 3-min denaturation at 94 C, 30 cycles of denaturation (94 C, 30 sec), annealing (55 C, 45 sec), and extension (72 C, 90 sec) with a 4-min extension after the last cycle. Two species were amplified with a 50 C annealing temperature (*E. barbouri, E. percnurum*). The PCR products were isolated with the Wizard Prep kit (Promega Corp.) or with ultrafiltration in a polysurfone tube (Millipore Corp.). The fragments were ligated into pGEM-T vector plasmids (Promega Corp.), and the plasmids were transformed into DH5-alpha–*Escherichia coli.* Plasmids from positive colonies were isolated with alkaline lysis using the PerfectPrep kit (5 Prime–3 Prime, Inc.) and used as template in sequencing reactions.

Cycle sequencing was conducted with one of the following kits: Delta-Taq Cycle Sequencing (Amersham), Amplicycle Sequencing (Perkin-Elmer), Thermosequenase Cycle Sequencing (Amersham). Internal primers were designed from alignments of sequences obtained with the PCR primers (Table 1). Forward and reverse strands were sequenced from different clones, and ambiguities were resolved by sequencing a

third clone. Sequencing products were electro-phoresed on two 6% polyacrylamide/8.3M urea gels (SequaGel Sequencing System, National Diagnostics), and the sequences were visualized with autoradiography. Portions of the cytochrome *b* gene for some species were sequenced by the University of Illinois Center for Biotechnology Genetic Engineering Facility, where cloned plasmids were used as template in fluorescent dye terminator sequencing reactions with Amplitaq FS kit (Perkin-Elmer). Sequences were determined with an ABI 373 Automated Sequencer and read from chromatograms. Consensus sequences were obtained with Sequencher (Gene Codes, Ann Arbor, MI) and aligned with Clustal V (Higgins et al., 1992).

Molecular phylogenetic analyses.—Pairwise sequence divergences, transition and transversion ratios, and percent nucleotide composition were calculated to examine patterns of variation in cytochrome *b* for the 18 species of *Catonotus*. Saturation was investigated through plots of positional substitutions against sequence divergences (e.g., Lydeard and Roe, 1997).

Phylogenetic trees were obtained with PAUP* (vers. 4.0.0d64, D. L. Swofford, 1998, unpubl.) under maximum-parsimony and maximum-likelihood criteria. All parsimony analyses employed a heuristic algorithm with tree-bisection-reconnection branch-swapping and the MULPARS (save all optimal trees) option in effect, and starting trees were obtained with 100 replicates of random stepwise addition. The g_1-statistic (Hillis and Huelsenbeck, 1992) was calculated by generating 10,000 random trees and comparing their lengths. The robustness of inferred nodes was assessed with a bootstrap analysis (2000 replicates) and a decay analysis (Bremer, 1988). Maximum-likelihood analysis invoked the following options: assumed nucleotide frequencies estimated from the data, number of substitution types set at two, and rates assumed to follow a gamma distribution with the alpha shape parameter and proportion of invariable sites estimated with maximum likelihood. The HKY85 model (Hasegawa, et al., 1985) with rate heterogeneity was used, with the transition:transversion ratio estimated with maximum likelihood and starting branch lengths obtained using the Rogers-Swofford approximation. Heuristic searches were used to find the topology with the best likelihood score using tree bisection-reconnection (TBR) with steepest descent option and 20 random additions. Bootstrap analysis of the maximum likelihood topology employed 200 replicates. Parsimony analysis was executed on two datasets with differing tax-onomic sampling. The first (37 species) included the 18 *Catonotus* species plus 19 other percids (Song et al., 1998). The second (20 species) included all species of *Catonotus*, *E. podostemone* and *E. vitreum*. *Etheostoma podostemone* and *E. vitreum* were included as outgroups because they were found in the analysis of all 37 percids to be most closely related to *Catonotus*. Maximum-likelihood analysis was executed using this second dataset.

To assess whether trees obtained with different optimization criteria differed statistically from each other, reciprocal comparisons of tree scores were made using both a pairwise parsimony method modified from the Templeton (1983) test (M-T) and the Kishino and Hasegawa (1989) test (K-H test) as implemented in PAUP*. Using the M-T test, trees were compared by testing for significantly longer tree lengths; this test calculates the difference in length between two trees and tests whether it is significantly different from zero based on the number of informative sites. K-H tests were utilized in comparing alternative hypotheses under maximum likelihood optimality criteria. The following alternative topologies were examined: parsimony cytochrome *b* tree, morphological tree (synonymous with trees in Page (1985) and Page et al. (1992)), Braasch and Mayden (1985) morphological tree, and the maximum–likelihood DNA tree. Some topologies recovered in total evidence analyses were not compared to maximum-parsimony and maximum-likelihood trees because of differences in taxonomic composition of the analyses.

Morphological data and analyses.—All morphological characters (and one behavioral character) presented by Page (1985), Braasch and Mayden (1985), and Page et al. (1992) were reassessed and coded for the 18 species of *Catonotus* and for the outgroup taxa, *E. podostemone* and *E. vitreum*. *Etheostoma podostemone* and *E. vitreum* were used as outgroups so comparisons could be made with results of the molecular analyses. Outgroup taxa were selected based on the results of molecular analyses. Characters such as meristic counts that are highly variable intraspecifically were excluded. The resulting dataset included 19 morphological characters and one behavioral character (Table 2, Appendix). All multistate characters except numbers 14 and 16 were ordered; justification for these assumptions of character evolution were presented in Page et al. (1992). The characters were analyzed with maximum parsimony criteria using the branch-and-bound algorithm in PAUP*. The ro-

TABLE 2. DATA MATRIX OF 20 MORPHOLOGICAL CHARACTERS USED FOR PHYLOGENETIC ANALYSIS OF *Catomotus* SPECIES. Character descriptions are presented in the Appendix.

Character	1	2	3	4	5	6	7	8	9	10	11	12	13	14	15	16	17	18	19	20
E. parvipinne	0	0	0	0	0	0	0	0	0	0	0	0	0	0	0	0	0	0	0	0
E. podostemone	0	0	0	0	0	0	0	0	0	0	0	0	0	0	0	0	0	0	0	0
E. vitreum	0	0	0	0	0	0	0	0	0	0	0	0	0	0	0	0	0	0	0	0
E. olivaceum	1	1	1	1	0	0	0	0	0	1	0	1	0	1	0	2	0	0	1	1
E. nigripinne	1	1	1	0	0	0	0	0	0	1	0	1	0	2	0	2	1	0	1	1
E. corona	1	1	1	0	0	0	0	0	0	1	0	1	0	2	0	2	1	0	1	1
E. forbesi	1	1	1	0	0	0	0	0	0	1	0	1	0	2	0	2	1	0	1	1
E. crossopterum	1	1	1	0	0	0	0	0	0	1	0	1	1	1	0	2	1	0	1	1
E. squamiceps	1	1	1	0	0	0	0	0	1	1	0	1	1	1	1	2	1	0	1	1
E. chienense	1	1	1	0	0	0	0	0	1	1	0	2	1	3	1	2	0	0	1	1
E. pseudovulatum	1	1	1	0	0	0	0	0	1	1	1	2	1	3	2	2	1	0	1	1
E. neopterum	1	1	1	0	0	0	0	0	1	1	2	2	1	4	2	2	0	0	1	1
E. oophylax	1	1	1	0	0	0	0	0	1	1	2	2	1	4	2	2	0	0	1	1
E. flabellare	1	1	0	0	0	1	0	1	0	3	2	0	0	0	0	2	2	0	2	2
E. kennicotti	1	1	0	0	0	1	0	1	0	2	0	0	0	0	0	2	2	0	2	2
E. percnurum	1	1	0	0	0	1	0	1	0	3	0	0	0	0	0	2	2	0	2	2
E. obeyense	1	1	0	1	1	1	1	1	0	1	0	0	0	0	0	0	2	0	2	2
E. virgatum	1	1	0	1	1	1	1	1	0	1	0	0	0	0	0	0	2	0	2	2
E. striatulum	1	1	0	1	1	1	1	1	0	1	0	0	0	0	0	0	2	1	3	2
E. barbouri	1	1	0	1	1	1	1	1	0	1	0	0	0	0	0	0	2	1	3	2
E. smithi	1	1	0	1	1	1	1	1	0	1	0	0	0	0	0	0	2	1	3	2

TABLE 3. DESCRIPTIVE STATISTICS (MEAN ± STANDARD ERROR) FOR A COMPLETE CYTOCHROME *b* DATASET OF 18 INGROUP TAXA.

	First position (380 base pairs)	Second position (380 base pairs)	Third position (380 base pairs)	All positions (1140 base pairs)
Uncorrected pairwise sequence divergence	4.6 ± 0.2 %	1.4 ± 0.1 %	36.7 ± 0.7 %	14.2 ± 0.3 %
Number of transitions	14.1 ± 0.53	4.0 ± 0.25	105.8 ± 1.84	123.9 ± 2.30
Number of transversions	3.2 ± 0.19	1.4 ± 0.10	33.8 ± 0.92	18.4 ± 1.04
TS:TV ratio	5.3 ± 0.28	2.6 ± 0.17	3.6 ± 0.14	3.7 ± 0.17
Number of variable positions	69	31	341	441
Number of informative positions	34	8	295	337

bustness of the resulting trees was assessed with bootstrap and decay analyses.

Total evidence analyses.—Two methods were used to assess congruence between the cytochrome *b* and the morphological datasets. First, the partition-homogeneity test (Farris et al., 1995), conducted with PAUP*, tests the null hypothesis that the sum of the lengths of the trees obtained from separate analyses does not differ from the sum of the lengths of the trees obtained from random partitions of the same data. The dataset included 361 variable, nonautapomorphic molecular characters and the 20 morphological/behavioral characters, and the test involved 100 replicates. Second, M-T and K-H tests were used to compare tree lengths between topologies obtained from separate analysis of molecular and morphological data (see above).

A dataset including the species of *Catonotus* (except *E. neopterum* because evidence suggested that the sequence data for that species represented introgressed mtDNA; see below) and up to three outgroups (*E. podostemone, E. vitreum,* and *E. parvipinne*) was used in total evidence analyses of 361 informative molecular (337 characters informative about ingroup relationships and 24 characters only supporting the monophyly of the subgenus) and 20 morphological characters. The maximum parsimony analysis used a heuristic algorithm with tree-bisection-reconnection branch-swapping and the MULPARS (save all optimal trees) option in effect, and starting trees were obtained with 100 replicates of random stepwise addition. Branch support was assessed with bootstrap (2000 replicates) and decay analysis. Consistency indices were calculated for the morphological characters and for each codon position in cytochrome *b*.

Although no trees are presented from datasets with characters of unequal weight, some analyses were conducted with weighted morphological characters to determine at what weights re-lationships supported by morphological data alone were obtained over relationships supported by molecular data. These analyses were conducted as above, except branch support was assessed with only 100 bootstrap replicates due to the large number of analyses performed.

RESULTS AND DISCUSSION

Cytochrome b.—Of 1140 base positions in the cytochrome *b* gene, 337 were phylogenetically informative about relationships among *Catonotus* species. For these 18 species, uncorrected pairwise sequence divergences ranged from 2.4–19.8% (mean = 14.2%), and most of the substitutions (77% of the 441 variable sites) occurred at the third codon position (Table 3). Transitions outnumbered transversions at all positions, and the overall transition:transversion ratio calculated from pairwise comparisons was about 3.7 (Table 3).

Plots of the numbers of transitions and transversions against genetic distance provided no strong evidence of saturation (Fig. 1). At the first and third codon positions, both transitions and transversions increased linearly relative to sequence divergence. At the second codon position, an increase was also seen although it is based on a small number of total substitutions. Lydeard and Roe (1997) noted similar substitution patterns using a cytochrome *b* dataset composed of 31 actinopterygian and six outgroup taxa.

Examination of the amino acid sequences for all *Catonotus* species found no stop codons in the cytochrome *b* gene. Of the 380 amino acid positions in cytochrome *b*, 66 were variable, and 43 of these were autapomorphies; most of the substitutions in this dataset resulted in silent (synonymous) changes. All of the *Catonotus* species exhibited a relatively low proportion of guanine, as is typical of cytochrome *b* (Lydeard and Roe, 1997). Means of the base frequencies for

A. Genetic distance at the first position

B. Genetic distance at the second position

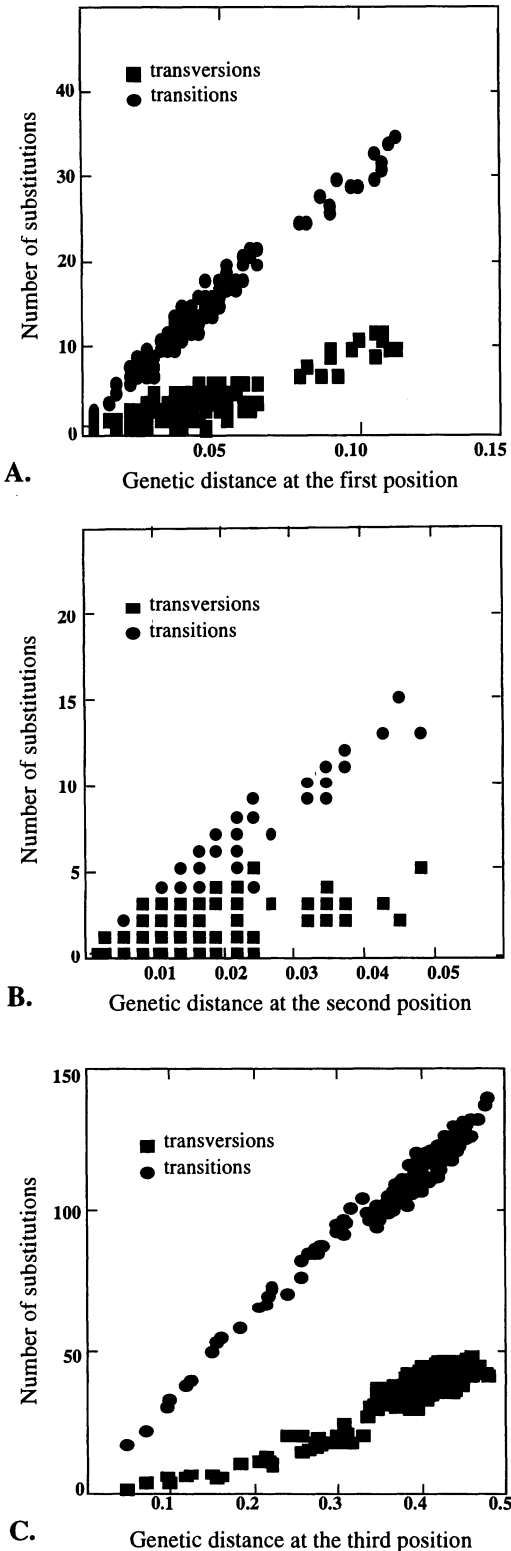**C.** Genetic distance at the third position

Fig. 1. Numbers of transitions and transversions versus uncorrected pairwise genetic distance for 153 comparisons among 18 species of *Catonotus*. (A) First codon position, (B) second codon position, (C) third codon position.

the 18 species were as follows: guanine, 0.170; adenine, 0.226; thymine, 0.297; cytosine, 0.307. A chi-square test of homogeneity of base frequencies among species showed no significant differences ($\chi^2 = 16.57$, df = 51, $P = 1.0$).

Molecular phylogenetic analyses.—Both datasets (37 and 20 species) analyzed under maximum parsimony criteria resulted in distributions of random trees that were significantly left-skewed (g_1 of -0.56 and -0.70, respectively), indicating that the datasets contained phylogenetic structure (Hillis and Huelsenbeck, 1992). Each dataset resulted in two most parsimonious trees; the strict consensus trees are shown in Figures 2–3. Relationships among species of *Catonotus* were identical in both consensus trees except for the position of *E. barbouri*. Bootstrap and decay values showed strong support for many of the nodes.

The tree resulting from the maximum-likelihood analysis (Fig. 4; $-\ln = 7202.22$) of the 20-species dataset was recovered after estimating the gamma shape parameter (1.16), transition:transversion ratio (6.47), and the proportion of invariable sites (0.51). The ingroup relationships were identical to those obtained with parsimony analysis except that *E. virgatum* paired with *E. striatulum* + *E. smithi* rather than with *E. obeyense*. Comparison of tree lengths of the different topologies obtained from the cytochrome *b* dataset using maximum parsimony and maximum-likelihood optimality criteria showed no significant differences among topologies (Table 4).

This dataset supported a monophyletic *Catonotus* (Fig. 2), although monophyly is not strongly supported by a high bootstrap value. The monophyly of the *E. squamiceps* group (*E. chienense* to *E. squamiceps* in Figs. 2–4) is well supported, as is the monophyly of a clade including members of the *E. virgatum* and *E. flabellare* groups (all other *Catonotus* species). The recognition of two major clades within *Catonotus* agrees with previous hypotheses (Page 1985; Braasch and Mayden 1985). However, the monophyly of the *E. virgatum* and *E. flabellare* groups are disrupted by the positions of *E. barbouri* and *E. percnurum*, each of which tended to cluster (Figs. 2, 4) with the group other than that in which it has been traditionally placed and is most similar morphologically. One poten-

←

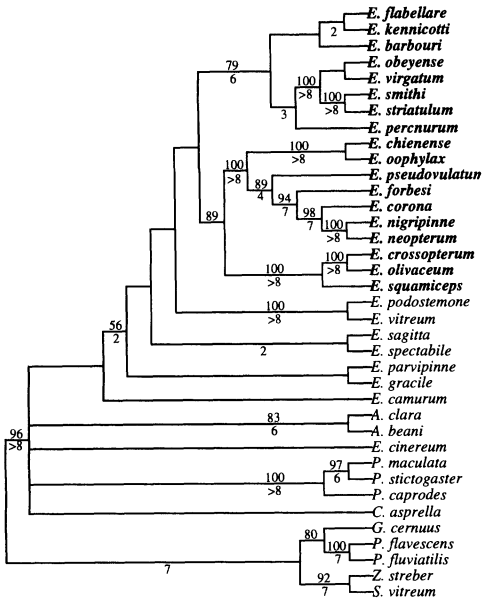codon position, (B) second codon position, (C) third codon position.

Fig. 2. Strict consensus of two most-parsimonious trees obtained with a heuristic search of the 37-species cytochrome *b* dataset [length = 3192, C.I. = 0.271 (excluding uninformative characters)]. Names in bold are species of *Catonotus*. The five nondarter percids (*G. cernuus* through *S. vitreum*) were designated outgroups. Numbers above branches indicate bootstrap support above 50% (2000 replicates); numbers below branches indicate decay values above 1.
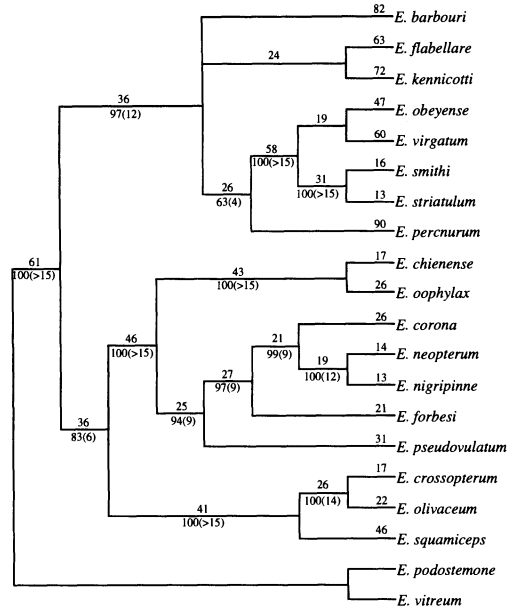
Fig. 3. Strict consensus of two most-parsimonious trees obtained with a heuristic search of the 20-species cytochrome *b* dataset [length = 1329, C.I. = 0.423 (excluding uninformative characters)]. *Etheostoma podostemone* and *E. vitreum* were designated outgroups. Numbers above branches represent branch lengths, and numbers below the branches indicate bootstrap support above 50% (2000 replicates) with decay values above 1 in parentheses.

tial problem encountered with parsimony analysis of highly divergent taxa is long branch attraction, or the grouping of taxa based on characters shared by chance and not by history (Felsenstein, 1978). *Etheostoma percnurum* and *E. barbouri* each possess many autapomorphies (branch lengths 90 and 82, respectively; Fig. 3). It is possible that these two species share fewer cytochrome *b* characters with close relatives due to history than they share with another species group because of increased homoplasy resulting from accelerated rates of evolution in these taxa.

Within the *E. squamiceps* group, two basal clades are robustly supported: one contains *E. crossopterum, E. olivaceum,* and *E. squamiceps*; and one contains the other seven species. Five members of the *E. squamiceps* group, *E. chienense, E. neopterum, E. oophylax, E. pseudovulatum,* and *E. squamiceps*, possess fleshy knobs on the ends of the second dorsal fin rays, although the knobs are much smaller in *E. squamiceps* than in the other species (Page et al., 1992). These knobs are thought to function as egg mimics, at least in the four species in which the knobs are large (Page and Swofford, 1984; Page et al., 1992). The cytochrome *b* data do not support the

monophyly of the five knob-bearing species or of the four species with large knobs. A sister relationship between one of the large-knobbed species, *E. neopterum,* and *E. nigripinne* is supported by the cytochrome *b* data; this pair of species exhibits a pairwise genetic distance of only 2.4%, a number which may be more characteristic of intraspecific variation in mitochondrial DNA (e.g., Nei, 1987; Avise, 1994). *Etheostoma nigripinne,* which is widespread in the Duck River and middle Tennessee River systems, occurs also in Shoal Creek, a small Tennessee River tributary system that encompasses the entire range of *E. neopterum.* The geographic distributions of these two species, the low level of divergence in cytochrome *b,* and the strong morphological resemblance of *E. neopterum* to *E. oophylax* (Page et al., 1992) and not to *E. nigripinne* suggest that the similarity between the cytochrome *b* genes of *E. neopterum* and *E. nigripinne* may be the result of introgression of *E. nigripinne* mtDNA into at least one population of *E. neopterum.*

Morphological data.—The morphological dataset was found to exhibit a significant left skew (g_1
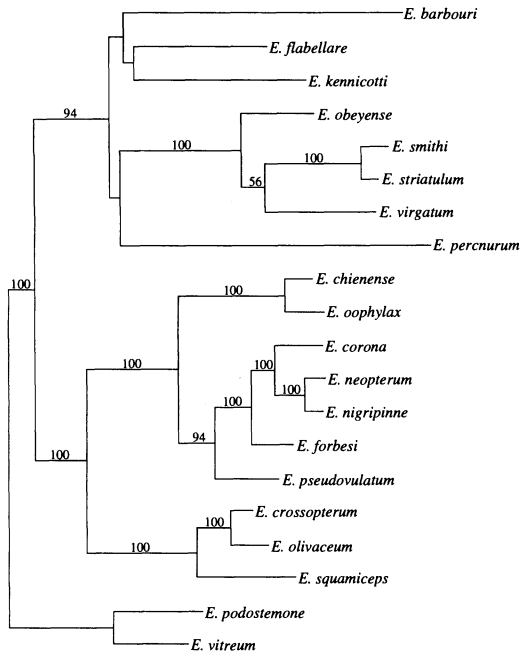
Fig. 4. Topology resulting from maximum likelihood analysis ($-\ln$ = 7202.22). Numbers above branches indicate bootstrap support above 50% (200 replicates).

= -0.517), and phylogenetic analysis of the 20 characters resulted in one most-parsimonious tree of 41 steps and a C.I. = 0.8 (Fig. 5). The four polytomies in this tree result from too few characters and not from character conflict; for example, no morphological characters support any sister-group relationship within the *E. forbesi*, *E. corona*, and *E. nigripinne* clade.

The phylogenetic relationships suggested by

the morphological data are similar to those obtained in the three previous studies (Page, 1985; Braasch and Mayden, 1985; Page et al., 1992). Relationships within the *E. squamiceps* group (*E. olivaceum* to *E. squamiceps* in Fig. 5) are identical to those proposed by Page et al. (1992), and the relationships among all species are the same as those presented by Page (1985), although the earlier study included only the 10 species of *Catonotus* described at that time. Several differences exist between the morphological tree presented here and that presented by Braasch and Mayden (1985). First, Braasch and Mayden (1985) supported a sister relationship between *E. barbouri* and *E. smithi* based on a reduction in the number of pored lateral line scales from >30% to >20%; the tree presented here shows a polytomy between these two species and *E. striatulum*. Second, Braasch and Mayden (1985) found *E. virgatum* to be sister to the *E. barbouri–E. smithi–E. striatulum* clade based on a reduction in pored lateral line scales, presence of longitudinal stripes on flanks, and presence of four scales above and eight scales below the lateral line. In the tree presented here, the sister taxon to the *E. barbouri–E. smithi–E. striatulum* clade is unresolved. Third, Braasch and Mayden (1985) supported a sister relationship between *E. crossopterum* and *E. nigripinne* based on modal number of pectoral fin rays and second dorsal fin pattern, and a sister relationship between these two species and *E. olivaceum* based on the black tips of the second dorsal fin rays. As depicted in Figure 5, *E. corona* and *E. forbesi* are more closely related to *E. nigripinne* than is *E. crossopterum*, and *E. olivaceum* is basal to all other members of the *E. squamiceps* group.

TABLE 4. PAIRWISE COMPARISONS BETWEEN ALTERNATIVE PHYLOGENETIC HYPOTHESES OF RELATIONSHIP AMONG THE SPECIES OF *Catonotus*. Each hypothesis in the left column was evaluated with three datasets (DNA, morphological, total evidence [TE]) using the parsimony-based modified Templeton test (M–T), and with the DNA dataset using a Kishino-Hasegawa test (K–H) of likelihood scores (MP = maximum parsimony, ML = maximum likelihood).

| Hypothesis	Cytochrome *b*	M–T test Tree lengths Morphological	Total evidence	Kishino-Hasegawa test $-\ln$ L Cytochrome *b*
DNA (MP 1) (also TE 1)	1,329 (best)	57**	1,272 (best)	7,207.045
DNA (MP 2) (also TE 2)	1,329 (best)	57**	1,272 (best)	7,205.209
DNA (ML)	1,331	57**	1,274	7,202.221 (best)
Morphology, Page (1985), Page et al. (1992)	1,556***	41 (best)	1,496***	7,658.029***
Morphology, Braasch and Mayden (1985)	1,624***	41	1,460***	7,712.155***

** = $P < 0.01$; *** = $P < 0.001$
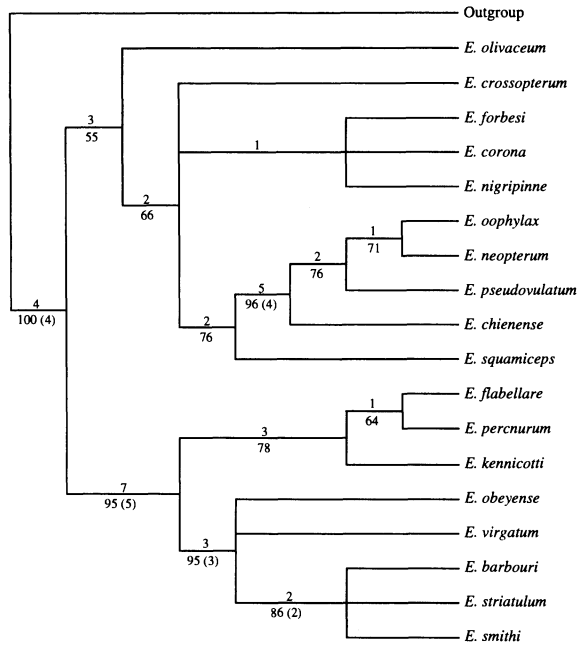
Fig. 5.   Most-parsimonious tree obtained from maximum-parsimony analysis (branch-and-bound algorithm) of 20 morphological characters [length = 41, C.I. = 0.825 (excluding uninformative characters)]. Numbers above branches represent branch lengths; numbers below branches indicate bootstrap support above 50% (2000 replicates) with decay values above 1 in parentheses.

Total evidence analysis.—To explore the congruence between molecular and morphological datasets, partition-homogeneity tests were conducted. This test compares the sum of the tree lengths from separate analyses of character partitions (in this case, molecular and morphological) with a distribution of tree-length sums based on 100 replicates of random partitions of the same data. The partition-homogeneity test was performed with a dataset that excluded *E. neopterum*, because that taxon may contain introgressed mtDNA; *E. podostemone* and *E. vitreum* were included in the dataset as outgroups. The molecular and morphological data were found to be significantly heterogeneous ($P = 0.05$), although four replicates resulted in tree length sums that were less than or equal to the sum of the tree lengths from separate analysis. In addition, a partition-homogeneity test conducted on a dataset excluding *E. barbouri* and *E. percnurum* (the two species with considerably longer branch lengths) found that the morphological and molecular datasets were no longer incongruent ($P = 0.27$). These results suggest that a total evidence analysis can provide additional insight into the phylogenetic relationships of *Catonotus*, although care should be taken in interpreting relationships that are in significant conflict between trees from separate molecular and morphological analyses.

Table 4 presents the results of the comparisons of all alternative topologies under both maximum-parsimony (cytochrome *b* and morphology) and maximum-likelihood (cytochrome *b* dataset) criteria. Results of the M-T tests (first three columns) clearly demonstrate that the molecular dataset does not support topologies obtained from analysis of morphological characters, and vice versa, as evidenced by the significantly different tree lengths. The same conclusions are drawn from results of the K-H tests, which compared likelihood scores of the same trees. Because these tests are constrained to a given topology per comparison, they may not address total dataset incongruence as effectively as the partition-homogeneity test; in other words, conflict in one part of the tree may override support for other relationships in the tree.

The total evidence parsimony analysis of 381 informative characters (361 molecular and 20 morphological) with *E. podostemone* and *E. vitreum* as outgroups resulted in two most-parsimonious trees that were identical to the two trees obtained with maximum-parsimony analysis of cytochrome *b* data. The strict consensus of the two total evidence trees is presented in Figure 6A.

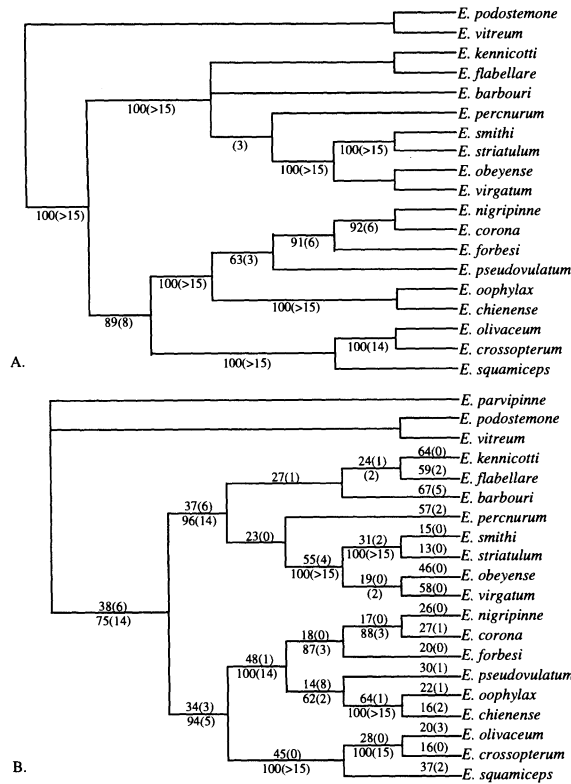An additional total evidence parsimony analysis was run with *E. parvipinne* added as an out-

Fig. 6. Results from total evidence analysis of 361 molecular and 20 morphological characters. (A) Strict consensus of two most-parsimonious trees resulting from analysis with *Etheostoma podostemone* and *E. vitreum* as outgroups [length = 1272, C.I. = 0.434 (excluding uninformative characters)]. (B) Most-parsimonious tree resulting from analysis with *E. parvipinne*, *E. podostemone*, and *E. vitreum* as outgroups [length = 1394, C.I. = 0.411 (excluding uninformative characters)]. Numbers above branches represent branch lengths with the number of molecular characters given first followed by the number of morphological characters in parentheses. Numbers below branches indicate bootstrap support above 50% (2000 replicates) with decay values above 1 in parentheses.

group taxon because an analysis of allozyme data (Wood and Mayden, 1997) suggested that *E. parvipinne* is closely related to *Catonotus*. The single most-parsimonious tree with *E. parvipinne* included (Fig. 6B) differed from the tree with only *E. podostemone* and *E. vitreum* as outgroups in the phylogenetic resolution of *E. barbouri* and in the placement of *E. pseudovulatum*. The phylogenetic placement of *E. pseudovulatum* with *E. chienense* and *E. oophylax* is of particular interest because all three species possess knobs on the second dorsal fin that are thought to function as egg mimics and because the monophyly of this clade is well supported by morphological data (Fig. 5). The numbers of molecular and morphological characters supporting each branch are shown in Figure 6B.

The tree in Figure 6B was used to calculate consistency indices for four character classes; second codon position changes were least homoplasious overall with a mean C.I. of 0.888. Mor-

phological characters exhibited a mean C.I. of 0.809, whereas first codon position changes had a mean C.I. of 0.762. Third position changes were most homoplasious with a mean C.I. of 0.497. Increased homoplasy of third codon position characters is explained by the increased rate of substitutions at that position although third position transversions were less homoplasious with a mean C.I. of 0.723. These data suggest that no one character class is considerably more consistent with the total evidence hypothesis and that a weighting scheme based on consistency indices (such as successive weighting; Farris, 1969) is not justified.

To further explore the interaction of the morphological and molecular datasets, a series of total evidence analyses involving weighted morphological characters was conducted. To obtain a monophyletic *E. flabellare* group (with bootstrap support >50%), the morphological data had to be weighted 3X, and to obtain a sister-

species relationship between *E. flabellare* and *E. percnurum*, the morphological data had to be weighted 10X. The morphological data had to be weighted 2X to obtain a monophyletic *E. virgatum* group and 13X to obtain a sister relationship between *E. barbouri* and *E. smithi* + *E. striatulum*. These analyses were conducted to evaluate how the large number of molecular characters compared with morphological characters contributed to the phylogenetic analysis. The morphological data had to be considerably weighted to obtain traditional relationships involving the highly autapomorphic taxa, *E. percnurum* and *E. barbouri* (10X and 13X, respectively).

Our combined analysis of morphological and molecular (cytochrome *b*) data resulted in a tree that is generally congruent with previous phylogenetic hypotheses. In particular, the *E. squamiceps* group and the *E. flabellare–E. virgatum* group are monophyletic. Also, within the *E. squamiceps* group, *E. chienense*, *E. pseudovulatum*, and *E. oophylax* (and, presumably, *E. neopterum*) form a monophyletic group (based on strong morphological evidence and one of the total evidence topologies), as do *E. nigripinne*, *E. corona*, and *E. forbesi*. Within the *E. virgatum* group, *E. smithi* and *E. striatulum* are sister species.

The monophyly of the *E. flabellare* group and that of the *E. virgatum* group are supported by convincing morphological synapomorphies (uniquely derived large yellow knobs on the first dorsal fin spines for the *E. flabellare* group, and the iridescent red and white cheek bar, blue-edged red fins on breeding males, and crenulate preopercle for the *E. virgatum* group). The lack of support for these species groups in the total evidence analysis is thought to be due to long-branch attraction resulting from the molecular data for *E. barbouri* and *E. percnurum*, as discussed above.

In contrast to earlier hypotheses, the total evidence analysis suggests that *E. squamiceps*, *E. crossopterum*, and *E. olivaceum* are closely related. The earlier hypothesis of Page, et al. (1992) suggested that *E. olivaceum* was basal to all other members of the *E. squamiceps* group and that *E. squamiceps* was related to *E. chienense*, *E. pseudovulatum*, *E. oophylax*, and *E. neopterum*. *Etheostoma olivaceum* was considered basal because it lacked putative synapomorphies of all other members of the *E. squamiceps* group: an interrupted infraorbital canal, 2–3 instead of 4 branches in each dorsal fin ray, and clear to yellow bands alternating with black bands on the caudal fin. The relationships of *E. squamiceps* to the *E. neopterum* group was based on two putative synapomorphies: adnate dorsal ray branches and a knob

of tissue at the tip of each dorsal ray. Although reversals (in *E. olivaceum*) and convergence (in *E. squamiceps*) of these character states are possible, a test of the two hypotheses of relationship requires additional data.

The results of all phylogenetic analyses conducted here suggest some interesting ideas about the combination of the molecular and morphological data available for the group, and about the use of total evidence approaches to phylogenetic analysis. Concerns about the utility of the morphological data for phylogeny reconstruction led to the addition of a molecular dataset for the subgenus *Catonotus*. Analysis of the molecular data raised some concerns about traditional relationships within *Catonotus*, such as the relationships of *E. olivaceum*, *E. pseudovulatum*, and *E. squamiceps*. These findings spurred reconsideration of the morphological data and demonstrated that all data are open to reinterpretation. However, problems arising from homoplasy due to long branch lengths (in *E. barbouri* and *E. percnurum*) led to a reliance on the morphological data for guidance in hypothesizing relationships and supported the contention that understanding the molecular data is crucial to performing appropriate analyses and drawing appropriate conclusions (Naylor and Brown, 1998). Regardless of the amount of data available for phylogenetic analysis of a particular group, a careful understanding of all types of data as well as knowledge of the organisms themselves is an important component in the development of phylogenetic hypotheses.

MATERIAL EXAMINED

Localities with GenBank accession numbers in parentheses for species sequenced during this study. Data for other species are given in Song et al. (1998). *Etheostoma barbouri*, INHS 27864, Price Creek (Green River), KY, 1 April 1992 (AF123028). *E. chienense*, INHS 48198, Bayou du Chien (Mississippi River), Hickman Co., KY, March 1990 (AF123029). *E. corona*, INHS 48192, Little Cypress Creek (Tennessee River), Wayne Co., TN, 11 April 1997 (AF123030). *E. crossopterum*, INHS 37848, East Fork Stones River (Cumberland River), Cannon Co., TN, 12 April 1996 (AF123031). *E. forbesi*, INHS 37909, Duke Creek (Caney Fork–Cumberland River), Cannon Co., TN, 12 April 1996 (AF123032). *E. neopterum*, INHS 48191, Butler Creek (Tennessee River), Wayne Co., TN, 11 April 1997 (AF123033). *E. nigripinne*, INHS 38583, Sinking Creek (Duck River–Tennessee River), Bedford Co., TN, 15 March 1996 (AF123034). *E. obeyense*, INHS 48194, Dutch Creek (Cumberland River),

Cumberland Co., KY, 4 May 1997 (AF123035). *E. olivaceum*, INHS 48197, Rock Springs Branch (Caney Fork–Cumberland River), Putnam Co., TN, 3 May 1997 (AF123036). *E. oophylax*, INHS 40861, Ledbetter Creek (Tennessee River), Calloway Co., KY, 31 March 1997 (AF123037). *E. parvipinne*, INHS 48195, trib., Powell Creek (Obion River), Weakley Co., TN, 6 August 1988 (AF123044). *E. percnurum*, INHS 48196, Copper Creek (Clinch River), Scott Co., VA, 6 August 1988 (AF123038). *E. pseudovulatum*, INHS 36029, Big Spring Creek (Duck River), Hickman Co., TN, 3 April 1995 (AF123039). *E. smithi*, INHS 28316, Ferguson Creek (Cumberland River), Livingston Co., KY, 5 April 1992 (AF123040). *E. squamiceps*, INHS 48199, Big Creek (Ohio River), Hardin County, IL, 28 October 1988 (AF123041). *E. striatulum*, INHS 48193, Hurricane Creek (Duck River), Bedford Co., TN, 11 April 1997 (AF123042). *E. virgatum*, INHS 27832, Roundstone Creek (Rockcastle River), Rockcastle Co., KY, 1 April 1992 (AF123043).

LITERATURE CITED

ALVES-GOMES, J.A., G. ORTI, M. HAYGOOD, W. HEILIGENBERG, AND A. MEYER. 1995. Phylogenetic analysis of the South American electric fishes (order Gymnotiformes) and the evolution of their electrogenic system: a synthesis based on morphology, electrophysiology, and mitochondrial sequence data. Mol. Biol. Evol. 12:298–318.

AVISE, J.C. 1994. Molecular markers, natural history and evolution. Chapman and Hall, New York.

BAILEY, R. M., AND W. A. GOSLINE. 1955. Variation and systematic significance of vertebral counts in the American fishes of the family Percidae. Misc. Publ. Mus. Zool. Univ. Mich. 93:1–44.

BART JR., H. L., AND L. M. PAGE. 1991. Morphology and adaptive significance of fin knobs in egg-clustering darters. Copeia 1991:80–86.

BRAASCH, M. E., AND R. L. MAYDEN. 1985. Review of the subgenus *Catonotus* (Percidae) with descriptions of two new darters of the *Etheostoma squamiceps* species group. Occ. Pap. Mus. Nat. Hist. Univ. Kans. 119:1–83.

———, AND L. M. PAGE. 1979. Systematic studies of darters of the subgenus *Catonotus* (Percidae), with the description of a new species from Caney Fork, Tennessee. *Ibid.* 78:1–10.

BREMER, K. 1988. The limits of amino acid sequence data in angiosperm phylogenetic reconstruction. Evolution 42:795–803.

BULL, J. J., J. P. HUELSENBECK, C. W. CUNNINGHAM, D. L. SWOFFORD, AND P. J. WADDELL. 1993. Partitioning and combining data in phylogenetic analysis. Syst. Biol. 42:384–397.

DIMMICK, W. W., AND A. LARSON. 1996. A molecular and morphological perspective on the phylogenetic relationships of the otophysan fishes. Mol. Phyl. Evol. 6:120–133.

FARRIS, J. S. 1969. A successive approximations approach to character weighting. Syst. Zool. 18:374–385.

———, M. KALLERSJO, A. G. KLUGE, AND C. BULT. 1995. Constructing a significance test for incongruence. Syst. Biol. 44:570–572.

FELSENSTEIN, J. 1978. Cases in which parsimony and compatibility methods will be positively misleading. Syst. Zool. 27:401–410.

HASEGAWA, M., H. KISHINO, AND T. YANO. 1985. Dating the human-ape splitting by a molecular clock of mitochondrial DNA. J. Mol. Evol. 22:160–174.

HIGGINS, D. J., A. G. BLEASBY, AND R. FUCHS. 1992. CLUSTAL V: improved software for multiple sequence alignment. Comput. Appl. Biosci. 8:189–191.

HILLIS, D. M. 1987. Molecular versus morphological approaches to systematics. Annu. Rev. Ecol. Syst. 18:23–42.

———, AND J.P. HUELSENBECK. 1992. Signal, noise, and reliability in phylogenetic analyses. J. Hered. 83:189–195.

———, B. K. MABLE, AND C. MORITZ. 1996. Applications of molecular systematics: the state of the field and a look to the future, p. 515–543. *In:* Molecular systematics. 2d ed. D. M. Hillis, C. Moritz, and B. K. Mable (eds.). Sinauer Associates, Inc., Sunderland, MA.

HUELSENBECK, J. P., J. J. BULL, AND C. W. CUNNINGHAM. 1996. Combining data in phylogenetic analysis. Trends Ecol. Evol. 11:152–158.

JENKINS, R. E., AND N. M. BURKHEAD. 1994. Freshwater fishes of Virginia. American Fisheries Society, Bethesda, MD.

KISHINO, H., AND M. HASEGAWA. 1989. Evaluation of the maximum likelihood estimate of the evolutionary tree topologies from DNA sequence data, and the branching order in Hominoidea. J. Mol. Evol. 31:151–160.

KLUGE, A. G. 1989. A concern for evidence and a phylogenetic hypothesis of relationships among *Epicrates* (Boidae, Serpentes). Syst. Zool. 38:7–25.

KNAPP, R. A., AND R. C. SARGENT. 1989. Egg-mimicry as a mating strategy in the fantail darter, *Etheostoma flabellare*: females prefer males with eggs. Behav. Ecol. Sociobiol. 25:321–326.

KUEHNE, R. A., AND J. W. SMALL JR. 1971. *Etheostoma barbouri*, a new darter (Percidae, Etheostomatini) from the Green River with notes on the subgenus *Catonotus*. Copeia 1971:18–26.

LARSON, A. 1994. The comparison of morphological and molecular data in phylogenetic systematics, p. 371–390. *In:* Molecular ecology and evolution: approaches and applications. B. Schierwater, B. Streit, G. P. Wagner, and R. DeSalle (eds.). Birkhauser Verlag, Basel, Switzerland.

LYDEARD, C. A., AND K. ROE. 1997. The phylogenetic utility of the mitochondrial cytochrome *b* gene for inferring relationships among actinopterygian fishes, p. 285–303. *In:* Molecular systematics of fishes. T. D. Kocher and C. A. Stepien (eds.). Academic Press, San Diego, CA.

MAYDEN, R. L. 1985. Nuptial structures in the subgenus *Catonotus*, genus *Etheostoma* (Percidae). Copeia 1985:580–583.

MESSENGER, S. L., AND J. A. MCGUIRE. 1998. Morphology, molecules, and the phylogenetics of cetaceans. Syst. Biol. 47:90–124.

MICKEVICH, M. F., AND J. S. FARRIS. 1981. The implications of congruence in *Menidia.* Syst. Zool. 30: 351–370.

MIYAMOTO, M. M. 1996. A congruence study of molecular and morphological data for eutherian mammals. Mol. Phyl. Evol. 6:373–390.

NAYLOR, G. J. P., AND W. M. BROWN. 1998. *Amphioxus* mitochondrial DNA, chordate phylogeny, and the limits of inference based on comparisons of sequences. Syst. Biol. 47:61–76.

NEI, M. 1987. Molecular evolutionary genetics. Columbia Univ. Press, New York.

PAGE, L. M. 1975. Relations among the darters of the subgenus *Catonotus* of *Etheostoma.* Copeia 1975:782–784.

———. 1981. The genera and subgenera of darters (Percidae, Etheostomatini). Occ. Pap. Mus. Nat. Hist. Univ. Kans. 90:1–69.

———. 1985. Evolution of reproductive behaviors in percid fishes. Bull. Ill. Nat. Hist. Surv. 33:275–295.

———, AND H. L. BART JR. 1989. Egg-mimics in darters (Pisces: Percidae). Copeia 1989:514–517.

———, AND D. L. SWOFFORD. 1984. Morphological correlates of ecological specialization in darters. Environ. Biol. Fish. 2:139–159.

———, P. A. CEAS, D. L. SWOFFORD, AND D. G. BUTH. 1992. Evolutionary relationships within the *Etheostoma squamiceps* complex (Percidae; subgenus *Catonotus*) with descriptions of five new species. Copeia 1992:615–646.

POE, S. 1996. Data set incongruence and the phylogeny of crocodilians. Syst. Biol. 45:393–414.

SONG, C. B., T. J. NEAR, AND L. M. PAGE. 1998. Phylogenetic relations among percid fishes as inferred from mitochondrial cytochrome *b* DNA sequence data. Mol. Phyl. Evol. 10:343–353.

SWOFFORD, D. L. 1991. When are phylogeny estimates from molecular and morphological data incongruent? p. 295–333. *In:* Phylogenetic analysis of DNA sequences. M. M. Miyamoto and J. Cracraft (eds.). Oxford Univ. Press, Oxford.

TEMPLETON, A. R. 1983. Phylogenetic inference from restriction endonuclease cleavage site maps with particular reference to the humans and apes. Evolution 37:221–244.

WOOD, R. M., AND R. L. MAYDEN. 1997. Phylogenetic

relationships among selected darter subgenera (Teleostei: Percidae) as inferred from analysis of allozymes. Copeia 1997:265–274.

ILLINOIS NATURAL HISTORY SURVEY, 607 EAST PEABODY DRIVE, CHAMPAIGN, ILLINOIS 61820. PRESENT ADDRESS: (JCP) CENTRE COLLEGE, 600 WEST WALNUT STREET, DANVILLE, KENTUCKY 40422. E-mail: (JCP) porterf@centre. edu. Send reprint requests to JCP.

APPENDIX

Morphological characters used in the phylogenetic analysis of species of *Catonotus*. All multistate characters were ordered except characters 14 and 16.

1. Shape of genital papilla of female: 0 = tubular or conical; 1 = broad and flat.
2. Breeding males with swollen flesh on head and nape: 0 = absent; 1 = present.
3. Females and nonbreeding males with body pattern of brown mottling on a light tan background and vertical row of three black spots at caudal fin origin: 0 = absent; 1 = present.
4. Iridescent red and white cheek bar (best developed on breeding males): 0 = absent; 1 = present. 5. Blue-edged red fins on breeding males: 0 = absent; 1 = present.
6. Scales on anterior body (cheek, opercle, nape, prepectoral area): 0 = present; 1 = absent.
7. Edge of preopercle: 0 = smooth; 1 = crenulate (data from Braasch and Mayden, 1985).
8. Fleshy ridges on ventrolateral scales of breeding males: 0 = absent; 1 = present (data from Mayden, 1985).
9. Clear triangle on distal edge of each interradial membrane of first dorsal fin of breeding male: 0 = absent; 1 = present.
10. Breeding male first dorsal fin spines: 0 = without knobs; 1 = small white knob on tip of each spine; 2 = large yellow knob on tip of each spine formed by a fleshy mass succeeded by a series of fleshy folds (Bart and Page, 1991); 3 = large yellow knob on tip of each spine formed by a fleshy mass succeeded by a yellow spot and a semicircle of melanophores (Bart and Page, 1991)—states are ordered: 0 → 1 → 2,3.
11. Breeding male second dorsal fin membrane: 0 = extends nearly to tips of rays; 1 = extends about two-thirds distance from base of fin to tips of rays; 2 = extends one-half to two-thirds distance from base of fin to tips of rays (states are ordered: 0 → 1 → 2).
12. Number of branches in second dorsal fin ray (excluding first ray): 0 = 4; 1 = 3; 2 = 2 (states are ordered: 0 → 1 → 2).

13. Second and third branches of second dorsal fin ray adnate: 0 = no; 1 = yes.

14. Horizontal rows of marks on second dorsal fin of breeding males: 0 = absent; 1 = clear to yellow crescents; 2 = bars; 3 = ovals; 4 = windows (see Page et al., 1992).

15. Knobs on second dorsal fin rays of breeding males: 0 = absent; 1 = small white knobs on adnate branches of each ray; 2 = large yellow knobs on adnate branches of each ray (states are ordered: 0 → 1 → 2).

16. Banding pattern on caudal fin of breeding males: 0 = absent; 1 = vertical rows of clear to yellow crescents on black fin, crescents often joined to form thin bands; 2 = clear to yellow bands alternating with equal-sized black bands.

17. Infraorbital canal: 0 = uninterrupted; 1 = narrowly interrupted (0–1 pore missing); 2 = widely interrupted (2–4 pores missing).

18. Infraorbital canal pore 2: 0 = present; 1 = absent (i.e., only three pores in anterior segment of interrupted canal).

19. Posterior segment of infraorbital canal: 0 = 4 pores; 1 = 3 pores (5 missing); 2 = 2 pores (5 and 6 missing); 3 = 1 pore (5, 6, and 7 missing—states are ordered: 0 → 1 → 2 → 3).

20. Inverted spawning position: 0 = absent; 1 = male and female only briefly invert during spawning; 2 = female remains inverted for an extended period (states are ordered 0 → 1 → 2; see Page, 1975; Page, 1985).